OPEN

Self-Organized and Cu-Coordinated Surface Linear Polymerization

Qing Li[1], Jonathan R. Owens[4], Chengbo Han[2], Bobby G. Sumpter[1,3], Wenchang Lu[2,3], Jerzy Bernholc[2,3], V. Meunier[4,5], Peter Maksymovych[1], Miguel Fuentes-Cabrera[1,3] & Minghu Pan[1]

[1]Center for Nanophase Materials Sciences, Oak Ridge National Laboratory, Oak Ridge, TN 37831, USA, [2]Center for High Performance Simulation and Department of Physics, North Carolina State University, Raleigh, NC 27695, USA, [3]Computer Science and Mathematics Division, Oak Ridge National Laboratory, Oak Ridge, TN 37831, USA, [4]Department of Physics, Astronomy, and Applied Physics, Rensselaer Polytechnic Institute, Troy, NY 12180, [5]Department of Materials Science and Engineering, Rensselaer Polytechnic Institute, Troy, NY 12180.

We demonstrate a controllable surface-coordinated linear polymerization of long-chain poly(phenylacetylenyl)s that are self-organized into a "circuit-board" pattern on a Cu(100) surface. Scanning tunneling microscopy/spectroscopy (STM/S) corroborated by *ab initio* calculations, reveals the atomistic details of the molecular structure, and provides a clear signature of electronic and vibrational properties of the poly(phenylacetylene)s chains. Notably, the polymerization reaction is confined epitaxially to the copper lattice, despite a large strain along the polymerized chain that subsequently renders it metallic. Polymerization and depolymerization reactions can be controlled locally at the nanoscale by using a charged metal tip. This control demonstrates the possibility of precisely accessing and controlling conjugated chain-growth polymerization at low temperature. This finding may lead to the bottom-up design and realization of sophisticated architectures for molecular nano-devices.

R ecently, surface-confined molecular polymerization and condensation reactions have been recognized as an effective route to synthesize robust mesoscale molecular architectures with well-defined and controllable local order[1–4]. Compared to assemblies stabilized by van der Waals interactions and hydrogen bonding, covalent interactions bring enhanced thermodynamic stability to the supported structure, can template epitaxial growth of organic molecules, nanoparticles and may also enable efficient electronic and ionic transport within the molecular structures making them superior for molecular electronic[5] and sensing applications. The detailed role played by the supporting surface is yet to be understood in surface-confined polymerization[4], but it is generally assumed that the reduced freedom of the adsorbed organic molecules to move on the surface may reduce the activation barrier, and confine molecules in a thin layer to higher temperatures, thereby allowing low-dimensional polymerization to occur[6–8]. Certainly, the surface also modifies and templates the structure of the supported oligomers or polymers. However, so far the general guidance has been to mimic bulk-like condensation or polymerization reactions on the surface. The examples include Ulmann coupling reaction[9–11] (and its derivatives), carbonyls and aldehydes condensation with amines forming imine bonds[12], self-condensation of boronic acids[13] and others. Indeed, the intermolecular bonding in this case is taxonomically identical to that in the bulk.

In this article, we report the linear polymerization of phenylacetylene (PA) molecules on Cu(100). Our studies were motivated by the known Cu-catalyzed polymerization of phenylacetylene to form polyphenylacetylene[14,15]. However, somewhat to our surprise, the alkyne groups appear to be acidic already at 120 K on the Cu(100) surface, based on our indirect experimental evidence and interpretation. As a result, the polymerization reaction occurred not between the parent phenylacetylene molecules, but among the surface-bonded phenyl copper acetylide species. The polymer product in this case was an entirely unique structure with an allene backbone, covalent bonding to the copper surface, a "circuit-board" pattern on Cu(100) terraces, and a nominal contraction in excess of 10% along the polymerized chain compared to polyphenylacetylene. The calculated band structure, partial density of states (PDOS) and tunneling spectroscopy both indicate the possibility of metallic conductance within the organic layer, *i.e.* the formation of a hybrid dispersive state. Moreover, the nanoscale structure of the polymer could be flexibly manipulated by either thermal fluctuations or a charged tip. This study therefore highlights a potentially new strategy for surface-supported polymerization and condensation reactions, where both molecule-surface and intermolecular chemistry is invoked in the formation of extended molecular networks. The benefit here is not only to shape
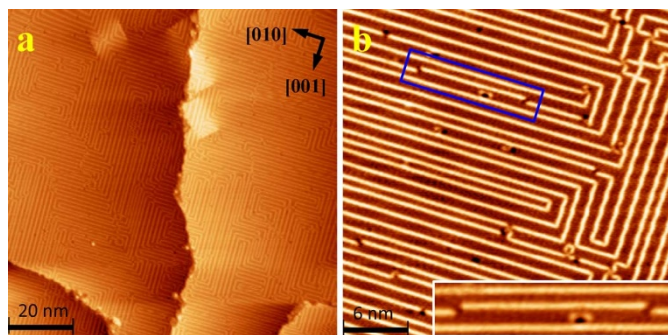
Figure 1 | Highly ordered self-assembled linear polymer on Cu(100). (a) Large scale scan shows a self-organized linear structure forming a "circuit-board" pattern all over the surface. (b) STM close-up image of the linear structure on Cu(100). Inset: A short section of the linear structure is displaced.

the structure uniquely, but also to create chemical bonding that can only be achieved on a metal-organic interface.

Results

One monolayer (ML) of PA molecules were deposited on a clean Cu(100) surface at 120 K under ultrahigh vacuum (UHV) conditions. Scanning tunneling microscopy (STM) imaging at 85 K revealed a self-assembled structure that resembles a "circuit-board" pattern (Fig. 1a and 1b). A large scale scan shows that this design forms uniformly over Cu(100) and is terminated only at step edges. By zooming into a small area, one can see that the pattern is

composed of bright lines spanning over several tens of nanometers (Fig. 1b). Those lines are well oriented along surface crystallographic directions, and are joined by 90° kinks. The linearity and overall topology of the structures is particularly distinct given the previous observations with PA molecules on the Au(111) surface[16,17]. Typically, an isolated PA molecule in the self-assembled architectures is identified as a pronounced elongated oval shape when it lies flat on a substrate, or relatively round and bright dots when it stands upright[16,17]. Such linear structures are thermally very stable, remaining intact even after annealing up to room temperature. Considering the facts described above, the observed lines are most consistent with the formation of a linear polymerized structure.

A high resolution STM image of the bright lines, acquired at a very low tunneling bias of 16 mV at 25 K, is shown in Fig. 2a (see Supplementary Information (SI) Fig. S1 for details). The lines have a periodic wavy microstructure, decorated with bright dots at both sides, and organized into an ordered array with two different lateral spacing, *e.g.* 0.91 nm and 1.28 nm (Fig. 2b). The unit cell along the stripe has a period of around 3.7 Å, corresponding to the lattice constant of Cu. The line structures are therefore epitaxial with the substrate lattice structure and orientated along the [001] and [010] directions of the Cu(100) surface.

Discussion

The observed wavy lines can be explained as a result of the polymerization of alkyne molecules[18–20]. The polymer backbone of polyphenylacetylene would correspond to that of polyacetylene, which in turn has two possible isomers *trans-* and *cis-*, with two and four monomers per unit cell, respectively. The *cis-*$(CH)_x$ polymerizes at
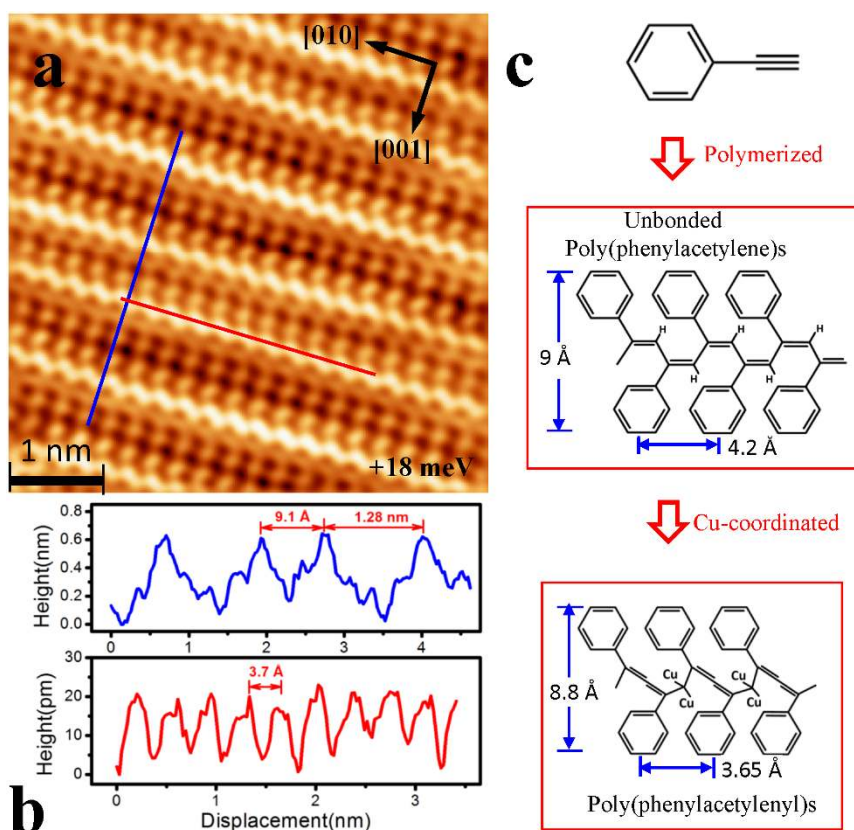

Figure 2 | Highly resolved STM image of the linear structure at very low bias. (a) Topographic image ($V_{bias} = +16$ meV, $I_{set} = 50$ pA) of linear structure showing the internal structure of polymer. (b) Height profiles for linear structures along horizontal and perpendicular directions. Both exhibit an identical structure with the periodicities of 3.65 Å along the chain and 9.1 Å/12.8 Å between the chains. (c) Chemical structure of *cis-*poly(phenylacetylene)s. The unbonded *cis-*poly(phenylacetylene)s in gas phase has a planar structure with the width of 9.0 Å, and a periodicity about 4.2 Å along the chain direction. With epitaxial bonding on the Cu substrate, *cis-*poly(phenylacetylene)s form a corrugated structure.
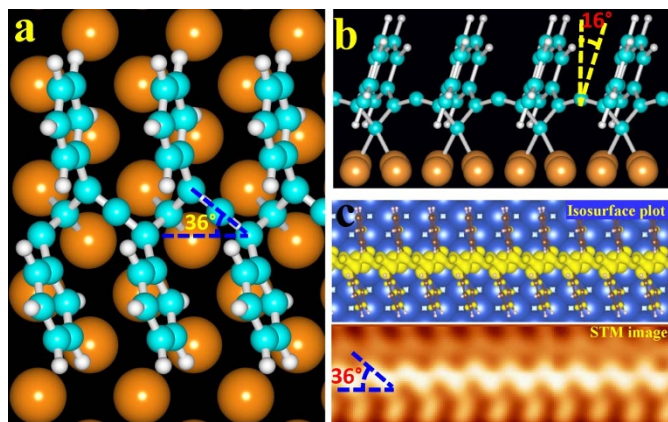
Figure 3 | The relaxed structure and the simulated STM image of the linear polymer from DFT calculations. (a) Top, (b) Side views of the calculated relaxed conformation for periodical cis-poly(phenylacetylene)s adsorbed on four layers of Cu(100), where cyan corresponds to carbon atoms, orange corresponds to the copper atoms of the substrate and light gray corresponds to hydrogen atoms. Buckling of the C-C backbone and surface reconstruction are clearly observed from side views. The middle copper atoms placed 0.03 Å below their equilibrium positions, the in-plane displacement between the copper atom and the unperturbed, unreconstructed equilibrium position is around 0.22 Å, whereas the C-C chain is buckled 0.16 Å out-of-plane in order to adopt the periodicity of 3.7 Å. (c) The high resolution STM topographic (lower panel) and the isosurface plot for a section of the polymerized structure (upper panel).

196 K on NaCl substrates, while trans-$(CH)_x$ can be obtained from the cis- isomer by annealing to $180°C^{21}$. To probe the feasibility of the cis-poly(phenylacetylene)s in our case, we used first-principles methods based on Density Functional Theory (DFT) to initially relax the structure in the gas phase. The width w of the relaxed poly(phenylacetylene)s chain (Fig. 2c) is about 0.90 nm, very close to the 0.91 nm (Fig. 2b) obtained experimentally. However, the unit-cell length between phenyl rings is 4.2 Å, which is significantly larger than the experimental value of 3.65 Å. Reducing the spacing to 3.65 A in the gas-phase requires about 1.6 eV in energy per PA molecule; Van der Waals interactions between the polymer and the Cu substrate are not strong enough to cause such a compression. An alternative model to simple polymerization of the alkyne groups would be to consider deprotonation of the alkyne group, and formation of the covalently anchored surface copper acetylide species. However, direct bonding of the phenylalkyne radical to the copper surface actually creates a hindrance to polymerization with the repeat-unit of Ph-C≡C•, because of the steric constraints and competition between intermolecular and molecule-surface bonding. DFT calculations reveal that this competition is resolved with a polymer backbone comprised of alternating allene (-C=C=C-) groups and sp^3-C atoms bonded directly to the two-fold Cu-Cu bridge site (Fig. 3a (top view), 3b (side view)). This polymerized structure accounts for all the structural features observed experimentally. The polymer is epitaxial with the Cu(100), and polymer chains are aligned along [001] and [010] directions. The unit cell has the periodicity of the Cu surface (3.65 Å) and the width of the polymer is 0.88 nm, both hold in very good agreement with the experiment observations. The rigidity of the allene fragment corrugates the polymer, inducing an asymmetric zig-zag carbon-carbon backbone. An isosurface plot of the integrated density of states within 0.7 eV above the Fermi level is shown in Fig. 3c (top panel), exhibiting a wavy C-C backbone, decorated with the phenyl rings as pendants, which matches quite well with the experimental STM image (bottom panel of Fig. 3c). Furthermore, the angle between the chain direction and the allene section is 36 ± 2° in the relaxed structure (Fig. 3a), same as that in the STM. Based on

this analysis, we conclude that phenylacetylene does not follow the anticipated bulk-like polymerization into polyphenylacetylene on Cu(100). Rather, the combination of molecule surface (deprotonation) and intermolecular (polymerization) covalent interactions produces a unique surface-supported polymer, with the backbone composed of allene fragments and sp^3 carbons bonded to copper.

One of the interesting properties of the surface-supported polymer in our case is the ease of manipulating the polymer chains by both "soft" (triggered by thermal fluctuation) and "hard" (triggered by high-voltage pulsing from STM tip) excitation. We note that owing to the steric constrains, the polymer covers approximately 2/3 of the surface area. The rest of the space (between bright lines) is occupied by Ph-C≡C• monomers, which gives rise to the two different spacing between the stripes: 0.91 nm and 1.28 (0.9 + 0.37) nm. Upon soft excitation at a relative high temperature (85 K), the polymerized structure can be manipulated by thermal fluctuation with the assistance of tip-induced excitation, leading to various dynamic behaviors of the "circuit-board" pattern, involving the shifting of half unit cell, extending/shrinking and complicate reorganizations. Such movement is demonstrated in a series of images during continuous scanning images (Fig. 4a, 4b and Fig. S2). We marked the [001] and [010] oriented stripes with different colors so that the evolution of the "circuit board" pattern can be highlighted. The observed clear movement of the architecture indicates depolymerization and subsequent repolymerization during soft excitation (Fig. S2). The detail of the mechanism and the energetics for soft excitation are still unclear.

On the other hand, at low temperature (28 K) where thermal fluctuation is not sufficient to lead to the manipulation of the polymer, hard excitation with the tip bias > 4 V causes depolymerization in significantly larger areas. Figure 4c shows a surface covered with a "circuit-board" pattern. We placed the STM tip at four different target positions, marked as stars in Fig. 4c, and applied a positively pulsed sample bias (+5 V) for 700 ms. Subsequent imaging at the same area (Fig. 4d) clearly shows the destruction of the polymer chain at the locations where the pulses were applied; the reacted region has a size of several nm^2 (Fig. 4d). Further scanning, with a positive sample bias (+4.5 V) applied from the top to half way from the bottom, leads to complete destruction of the lines within the scan range (Fig. 4e). A close-up STM image (Fig. 4f) reveals that the reacted regions have a four-fold symmetry close-packed structure with the nearest neighbor distance of 3.65 Å. It is worth noting that the reacted region cannot be attributed to the native lattice of Cu(100). The STM image of Cu(100) surface would show its 1 × 1 structure, with an atom spacing of 2.55 Å [22] and the atoms run along the [011] and [0$\bar{1}$1] direction. In our case, the spacing is 3.7 Å and the self-assembled structure run along [010] and [001] direction. Therefore, the reacted region implies a two-dimensional epitaxially anchored molecular structure.

Both soft and hard depolymerizations confirm the identity of the monomers as surface-bonded Ph-C≡C• species. In particular, this is required by the observed repolymerization. The exact structure of the monomer can only be attributed to the Ph-C≡C• bonded normal to the surface[23] (as opposed to flat-lying species and styrene derivatives, which would be incompatible with the observed dense packing, see SI, Fig. S3 for details). This means that deprotonation of phenylacetylene occurs already at a temperature of ~100 K, which supports our polymerization model based on the deprotonation. We have used DFT calculations to investigate the reaction barriers for the dehydrogenation process (see SI), which is a critical step for the polymerization reaction based on our model. These calculations indicate that dehydrogenation is energetically favorable and the energy drop from physisorbed phenylaceylene to a deprotonated radical species is as large as ~0.79 eV per PA molecule.

To investigate the electronic properties of the polymer, we calculated the band structure for chemisorbed poly(phenylacetylenyl)s on Cu(100), as shown in Fig. 5a. Strikingly, two hybrid bands arising
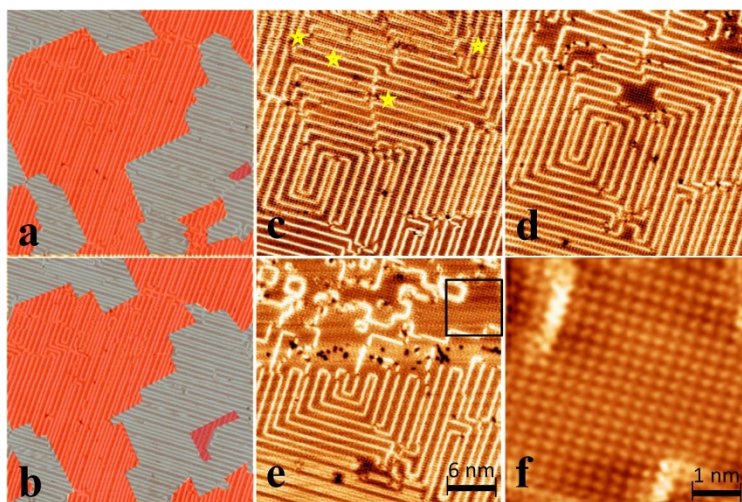
3

Figure 4 | Thermal-induced "soft depolymerization" and controllable depolymerization by STM tip. (a) and (b) Two STM images during the continuous scanning at 85 K. Stripes along [001] and [010] directions are marked with red and grey colors respectively. Tunneling current is 100 pA and the sample bias is set as +500 mV. (c) A target region in which "circuit board" pattern is formed. Marks are four positions that each voltage pulse is applied. (d) STM image of the region after the voltage pulse. (e) STM image of the region after scanning with +4.5 V sample bias. (f) A zoom-in image into reacted zone shows a four-fold close-packed molecule assembly.

primarily from the largely filled C(s,p) orbitals of the polymer and Cu(s,p) bands were found to cross the Fermi level. This calculation clearly suggests that the observed polymer is metallic due to the formation of dispersive hybrid surface-polymer states, which is distinct from the fact that most conjugated polymers are semiconductors[14,15]. We also calculated the corresponding PDOSs for poly(phenylacetylenyl)s bonding with copper (see SI). Accordingly, the PDOS (Fig. S4) shows a non-zero value around Fermi Level (E_F) from central chain of polymerized monomers. The PDOS near the Fermi level of the Cu bound poly(phenylacetylenyl)s is dominated by the polymerized fragments, with a negligible contribution from the phenyl groups (SI, bottom panels of Fig. S4). This explains the brightness of the contrast in the STM, even though topographically the phenyl groups are taller. This is also consistent with the fact that we can acquire a STM image at bias as low as 16 mV. Additionally, a

non-zero conductance around E_F observed in our dI/dV spectra strongly supports this conclusion (Inset of Fig. 5b).

This poly(phenylacetylenyl)s also exhibits unique vibrational property. The inelastic electron tunneling spectroscopy (IETS) technique based on STM technique, pioneered by Ho et al., can detect the molecular vibrational modes[24,25], and was used here to investigate the vibrational properties of the polymer. A pair of asymmetric peaks are observed in the low energy region ($\pm$ 16 mV) for the observed polymers (Fig. 5b), with exceeding 20% relative change in the differential conductance (Insert of Fig. 5b), much larger than the largest value (10%) reported for the C–H stretch mode in acetylene on Cu(100)[24,25]. By contrast, such vibrational peaks are not observed for a single phenylacetylene molecule and bare Cu(100) surface (Fig. 5b). The vibrational energy of 16 meV from IETS spectrum is well below the expected values for internal vibrations of a phenylacetylene molecule
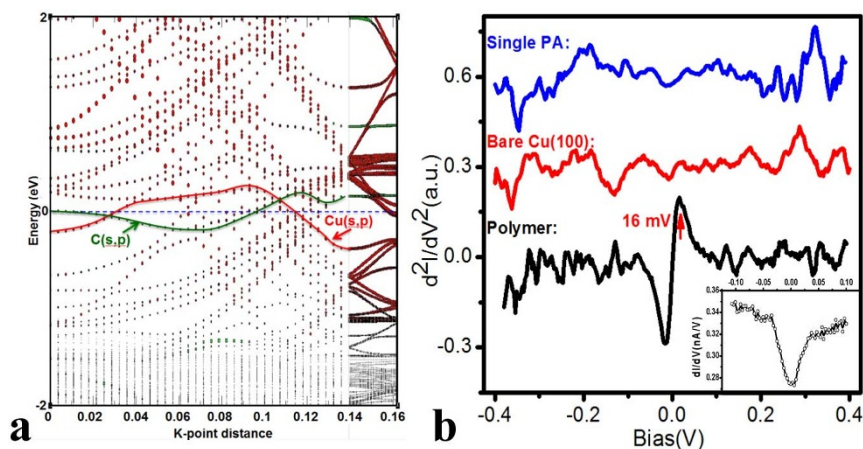

Figure 5 | Electronic structure and a distinct vibrational mode of the polymerized structure. (a) The computed band structure Band for the PA polymer on Cu(100). Two bands, shown in green and red, cross the Fermi level: these are contributed by C(s,p) and Cu(s,p) orbitals, respectively; (b) d^2I/dV^2 recorded directly over the bare Cu(100) surface (red), on a monolayer of adsorbed phenylacetylene molecule (blue) and over the cis-poly(phenylacetylene)s (black). The last spectrum shows a pair of asymmetric peaks at $\pm$ 16 mV. The area of the IETS peak gives the conductance change, Δs ($\Delta s/s \sim 20\%$), as well as the drop of the differential conductance (Inset figure). dI/dV from the lock-in amplifier recorded simultaneously with d^2I/dV^2 measurement over the cis-poly(phenylacetylene)s. The dI/dV spectrum (Inset) shows a sharp drop and increase at a sample bias of $\pm$ 16 mV (arrow). A sample bias modulation of 3 mV was used.

adsorbed on metal surface, indicating a larger oscillator mass. The vibrational frequency of a perpendicular stretch mode Z(molecule-Cu) was estimated by treating the polymer as a harmonic oscillator. The frequency is related to the molecular parameters by: $\varpi = \sqrt{\dfrac{k}{\mu}}$, where k is the bond force constant and μ the reduced mass. The force constant of C-Cu is comparable to a prototype adsorbate-substrate system—carbon monoxide on Cu(100) surface, which has been well studied both in experiments[26] and first principle calculations[27]. A vibration at frequency of 347 cm^{-1} (43 meV) was found for CO molecule adsorbed at top site, and it was attributed to a stretch mode. The lower vibrational frequency in our case reflects the heavier molecular mass, expected to be 202 *amu* from the formula; this number coincides with the weight of the formula per unit cell of our polymerized structure (C_8H_5). This observation reflects the nature of the polymer vibrating as a whole unit and supports our polymer model.

In summary, we have shown that combining surface-molecule and intermolecular polymerization on supported layers can produce a unique polymer structure that is exclusive to the metal-organic interface. In the case of phenylacetylene the acidity of the alkyne groups is sufficiently strong to cause deprotonation already at cryogenic temperatures. Subsequent intermolecular polymerization yields a polymer backbone based on allene fragments alternating with sp^3 carbon atoms anchored to the copper surface. The specifics of the bonding allows polymerization and depolymerization reactions to be readily triggered at the nanoscale by both thermal and tip-induced excitation. We can hypothesize that any alkyne polymerization on copper may follow a similar pathway. The surface-supported allene groups in the polymer backbone are also of interest for subsequent chemical reactivity of the supported polymer, which may lead to novel unique and non-bulk like supported polymer architectures for molecular nano-devices.

Methods

Sample and tip preparation. Sample preparation and STM measurements were performed in an ultrahigh vacuum system (base pressure is better than 1×10^{-10} mbar). Experiments were conducted with a home-built variable temperature scanning tunneling microscopy, whose temperature can vary from 25 K to 300 K. Phenylacetylene molecules were purified by the standard freeze-pump-thaw process. The Cu(100) surface was cleaned by standard argon sputtering-annealing cycles before deposition of phenylacetylene molecules. The Cu(100) substrate was kept at around 120 K during the molecular deposition. A commercial Pt-Ir tip was prepared by gentle field emission at a clean Cu(100) sample. The bias voltage was applied on the sample during the STM observations. The STM images were analyzed using WsXM[28].

DFT calculations. All the calculations were performed with the Vienna Ab-initio Simulation Package, VASP[29]. For the polymer in gas-phase, calculations were performed to determine the size of the unit cell. For this purpose, the unit cell size varied l from 3.3 to 4.6 Å. The calculations employed PAW pseudopotentials[30], the Perdew, Burke and Ernzerhof approximation (PBE)[31] for the exchange correlation interaction, an energy cutoff of 544 eV, and a $18 \times 1 \times 1$ k. The same method was used when the polymer was deposited on Cu(100), except the k-point mesh was increased to $18 \times 3 \times 1$, with a $3.64 \times 21.80 \times 25.46$ Å supercell. The polymer deposited on Cu(100) was relaxed using the same parameters. The Cu substrate consisted of 4 layers. During relaxation, the upper 3 layers of Cu and the polymer were allowed to move. The system was relaxed until the atomic forces were smaller than 0.02 eV/Å.

The simulated STM images of the optimized structure shown in Fig. S3b were obtained using the Tersoff's formalism[32], in which the current crucially depends on the local density of states (LDOS) of the surface sampled. To obtain the constant current STM image, the LDOS surface with the same value is recorded in a top view manner. The changes with height in the LDOS surface above the Cu(100) slab correspond to the tip retractions in the constant current mode STM measurement.

1. Perepichka, D. F. & Rosei, F. Extending polymer conjugation into the second dimension. *Science* **323**, 216–217 (2009).
2. Champness, N. R. Building with molecules. *Nat. Nanotech.* **2**, 671–672 (2007).
3. Gourdon, A. On-surface covalent coupling in ultrahigh vacuum. *Angew. Chem. Int. Ed.* **47**, 6950–6953 (2008).
4. Zhong, D. Y. *et al.* Linear alkane polymerization on a gold surface. *Science* **334**, 213–216 (2011).
5. Nitzan, A. & Ratner, M. A. Electron transport in molecular wire junctions. *Science* **300**, 1384–1389 (2003).
6. Ozaki, H., Funaki, T., Mazaki, Y., Masuda, S. & Harada, Y. Single sheet of a quasi-planar macromolecule prepared by a photopolymerization at a solid surface. *J. Am. Chem. Soc.* **117**, 5596–5597 (1995).
7. Sakaguchi, H., Matsumura, H. & Gong, H. Electrochemical epitaxial polymerization of single-molecular wires. *Nat. Mater.* **3**, 551–557 (2004).
8. Yang, L. Y. O., Chang, C., Liu, S., Wu, C. & Yau, S. L. Direct visualization of an aniline admolecule and its electropolymerization on Au(111) with in situ scanning tunneling microscope. *J. Am. Chem. Soc.* **129**, 8076–8077 (2007).
9. Lipton-Duffin, J. A., Ivasenko, O., Perepichka, D. F. & Rosei F. Synthesis of polyphenylene molecular wires by surface-confined polymerization. *Small* **5**, 592–597 (2009).
10. Blake, M. M. *et al.* Identifying reactive intermediates in the Ullmann coupling reaction by scanning tunneling microscopy and spectroscopy. *J Phys. Chem. A.* **113**, 13167–13372 (2009).
11. Zhang, Y. Q. *et al.* Homo-coupling of terminal alkynes on a noble metal surface. *Nat. Commun.* **3**, 1286 (2012).
12. Weigelt, S. *et al.* Surface synthesis of 2D branched polymer nanostructures. *Angew. Chem. Int. Ed.* **47**, 4406–4410 (2008).
13. Zwaneveld, N. A. A. *et al.* Organized formation of 2D extended covalent organic frameworks at surfaces. *J. Am. Chem. Soc.* **130**, 6678–6679 (2008).
14. Etemad, S., Heeger, A. J. & Macdiarmid, A. G. Polyacetylene, (CH)$_X$-the prototype conducting polymer. *Ann. Rev. Phys. Chem.* **33**, 443–469 (1982).
15. Macdiarmid, A. G. "Synthetic metals": A novel role for organic polymers (Nobel lecture). *Angew. Chem. Int. Ed.* **40**, 2581–2590 (2001).
16. Li, Q. *et al.* Supramolecular self-assembly of π-conjugated hydrocarbons via 2d cooperative CH/π interaction. *ACS Nano* **6**, 566–572 (2012).
17. Li, Q. *et al.* Electronic control over attachment and self-assembly of alkyne groups on gold. *ACS Nano* **6**, 9267–9275 (2012).
18. Mandal, S. K., Okawa, Y., Hasegawa, T. & Aono, M. Rate-determining factors in the chain polymerization of molecules initiated by local single-molecule excitation. *ACS Nano* **5**, 2770–2778 (2011).
19. Okawa, Y. & Aono, M. Nanoscale control of chain polymerization. *Nature* **409**, 683–684 (2001).
20. Giridharagopal, R. & Kelly, K. F. Substrate-dependent properties of polydiacetylene nanowires on graphite and MoS$_2$. *ACS Nano* **2**, 1571–1580 (2008).
21. Ito, T., Shirakawa, H. & Ikeda, S. Simultaneous polymerization and formation of polyacetylene film on surface of concentrated soluble Ziegler-type catalyst solution. *J. Polym. Sci. Polym. Chem. Ed.* **12**, 11–20 (1974).
22. Matsushima, H., Taranovskyy, A., Haak, C., Gründer, Y. & Magnussen, O. M. Reconstruction of Cu(100) electrode surfaces during hydrogen evolution. *J. Am. Chem. Soc.* **131**, 10362–10363 (2009).
23. Ford, M. J., Hoft, R. C. & McDonagh, A. M. Theoretical study of ethynylbenzene adsorption on Au(111) and implications for a new class of self-assembled monolayer. *J. Phys. Chem. B* **109**, 20387–20392 (2005).
24. Stipe, B. C., Rezaei, M. A. & Ho, W. Single-molecule vibrational spectroscopy and microscopy. *Science* **280**, 1732–1735 (1998).
25. Ho, W. Single-molecule chemistry. *J. Chem. Phys.* **117**, 11033–11061 (2002).
26. Philipsen, P. H. T., Tevelde, G. & Baerends, E. J. The effect of density-gradient corrections for a molecule-surface potential energy surface. Slab calculations of Cu(100)c(2 × 2)-CO. *Chem. Phys. Lett* **226**, 583–588 (1994).
27. Lewis, S. P. & Rappe, A. M. Structural and vibrational properties of carbon monoxide on the copper (001) surface. *J. Chem. Phys.* **110**, 4619–4633 (1999).
28. Horcas, I. *et al.* WSXM: a software for scanning probe microscopy and a tool for manotechnology. *Rev. Sci. Instrum.* **78**, 013705-1–013705-8 (2007).
29. Kresse, G. & Hafner, J. Ab initio molecular dynamics for liquid metals. *Phys. Rev. B* **47**, 558–561 (1993).
30. Blochl, P. E. Projector augmented-wave method. *Phys. Rev. B* **50**, 17953–17979 (1994).
31. Perdew, J. P., Burke, K. & Ernzerhof, M. Generalized gradient approximation made simple. *Phys. Rev. Lett.* **77**, 3865–3868 (1996).
32. Tersoff, J. & Harmann, D. R. Theory of the scanning tunneling microscope. *Phys. Rev. B* **31**, 805–813 (1985).

Acknowledgements

Author contributions

Q.L., P.M., M.P. performed STM measurements and analyzed STM data. C.H., J.O., M.F.C.,

W.L., J.B., V.M. and B.G.S. carried out theoretical calculations. All authors discussed the results and wrote the paper.

Additional information